Experimental Determination of Energy Disposal in the Dissociative Electron Recombinations of CS_2^+ and HCS_2^+

C. D. Molek, R. Plasil,† J. L. McLain, N. G. Adams,* and L. M. Babcock

Department of Chemistry, University of Georgia, Athens, Georgia 30602

Received: September 26, 2007; In Final Form: October 22, 2007

Vibronic optical emissions from CS($A^1\Pi \rightarrow X^1\Sigma^+$) and CS($a^3\Pi \rightarrow X^1\Sigma^+$) transitions have been identified from dissociative recombination (DR) of CS_2^+ and HCS_2^+ plasmas. All of the spectra were taken in flowing afterglow plasmas using an optical monochromator in the UV−visible wavelength region of 180−800 nm. For the CS($A \rightarrow X$) and CS($a \rightarrow X$) emissions, the relative vibrational distributions have been calculated for $v' < 5$ and $v' < 3$ in both types of plasmas for the CS(A) and CS(a) states, respectively. Both recombining plasmas show a population inversion from the $v' = 0$ to $v' = 1$ level of the CS(A) state, similar to other observations of the CS(A) state populations, which were generated using two other energetic processes. The possibility of spectroscopic cascading is addressed, such that transitions from upper level electronic states into the CS(A) and CS(a) states would affect the relative vibrational distribution, and there is no spectroscopic evidence supporting the cascading effect. Additionally, excited-state transitions from neutral sulfur ($S(^5S_2^0 \rightarrow {}^3P_2)$ and $S(^5S_2^0 \rightarrow {}^3P_1)$) and the products of ion−molecule reactions ($CS(B^1\Sigma^+ \rightarrow A^1\Pi)$, $CS^+(B^2\Sigma^+ \rightarrow A^2\Pi_i)$, and CS_2^+ ($\tilde{A}^2\Pi_u \rightarrow X^2\Pi_g$)) have been observed and are discussed.

1. Introduction

Dissociative electron-ion recombination (DR) is an important ionization loss process in many plasmas varying from the interstellar medium (ism) to those used as gas lasers.[1−8] In studies of this process, a considerable amount of effort has been devoted to determining the recombination rate coefficients, including a few as a function of temperature,[9−12] and more recently, effort has been directed to determining the neutral product (ground electronic state) distributions.[13−44] Since DR is an energetic process, often the products can be in electronically excited states. Information on the states populated, and vibrational excitation in these states, suggests reaction mechanisms and puts constraints on theory. For example the recombinations of N_2H^+ and N_2D^+ result in the population of the $N_2(B^3\Pi_g)$ state which undergoes a radiative transition to the $A^3\Sigma_u^+$ state.[45] Observation of these emissions, together with the known Franck−Condon factors for the transition, led to a determination of the vibrational population distribution of the B state populated in the recombinations. Comparison of the ratio of the population distributions produced with N_2H^+ and N_2D^+ has shown that the relative population of $v' = 6$ for N_2H^+ is enhanced by a factor of ~1.6 over the population for N_2D^+ at 300 K, increasing dramatically to 6 at 100 K.[11,46] The energy level for $v' = 6$ is closely resonant with the vibrational ground state ($v = 0$) of the recombining N_2H^+ ion and this accidental resonance strongly suggests a mechanism involving quantum tunneling through a barrier between the bound ionic potential surface and the repulsive dissociative curve to the products $N_2(B^3\Pi_g)$ and H. Such a scenario was suggested by Bates as a general possibility prior to this work.[47−49] Recently, potential energy curves (A and W) for the products N_2 + H have been calculated for the N_2H^+/e^- system.[50] Unfortunately, the N_2 B state crossing, was not calculated and therefore detailed information is still needed to determine the likelihood of the suggested tunneling mechanism. In addition, Rosati et al.[51] quantitatively assigned the total emission intensity from the measured $N_2(B \rightarrow A)$ with a yield 19% ± 8% originating from the $N_2(B, v' \geq 1)$.

There is also some indication of a tunneling mechanism in the case of the CO(a) state produced in the recombinations HCO^+/DCO^+.[46] However, it was not possible to determine the relative population of the resonant level (because of spectral line overlap) although there is some indication of an enhancement as this level is approached. Theoretical calculations are available for this system, although there is disagreement as to where the ion potential surface (represented as a curve) is crossed by the repulsive curve to ground state products.[52,53] No detailed information is available for dissociation to the CO(a) state; however, calculations with approximate potentials[54] have given reasonable agreement with the experimental vibrational distribution.

An example of the applied significance of these recombinations is the observation of CO ($a \rightarrow X$) Cameron band emissions from the Red Rectangle of the interstellar medium.[55] These show a CO (a) state vibrational population distribution very similar to that observed in the laboratory from the HCO^+ recombination. Yan et al.[56] have analyzed this situation in detail and concluded that this recombination is indeed the source of the interstellar emissions, the first time an individual chemical reaction has been observed outside the solar system. This lends strong independent support of the widely accepted view that interstellar chemistry is driven significantly by ionic reactions. This conclusion was previously based on the general agreement between overall model calculations and observed neutral abundances.

In addition, the observed sulfur content in the ism only contributes about 4% of the calculated cosmic abundance of

* Corresponding author. E-mail: adams@chem.uga.edu.
† Current address: Faculty of Mathematics and Physics, Charles University, V Holesovickach 2, Praha 8, 180 00, Czech Republic.

10.1021/jp0777420 CCC: $40.75
Published on Web 01/11/2008

sulfur.[57−59] How much CS_2 is contributing to the total cosmic abundance of sulfur is unknown, but recombination studies of CS_2^+ and HCS_2^+ could give insight into the existence of the molecule and possibly its contribution to the ism. Like CO_2, CS_2 is symmetrical, thus rendering it unobservable in the microwave and infrared regions available in the ISM, but recent work has proved the presence of CS_2 in comets by identification of UV emission lines.[60] In addition, CS and S have been observed in the ism[58] and cometary comae.[61] These are both products of the DR of CS_2^+, which may point to the existence of CS_2 in the ism.

In order to try to establish general trends in the DR process and also to gain knowledge about charge-transfer mechanisms of ion-neutral reactions (i.e., long range versus an intimate encounter) we have continued to investigate recombination emissions with studies of the CS_2^+ recombination analogue of CO_2^+ studied previously[62−64] and HCS_2^+, which is moving the studies to more complex protonated ions. This additionally enables the effect of the protonation on recombination to be assessed.

2. Experimental Section

The studies were performed using a flowing afterglow, the basic features of which have been described in detail previously,[65,66] and this detail will not be repeated here. Briefly, He is passed through a microwave discharge ionization source, and the plasma and remaining He proceeds along the flow tube to a downstream mass spectrometer under the action of a Roots pump. At a series of positions along the tube, measured flows of various reactant gases can be added and the chemical reactions monitored by the mass spectrometer/ion detection system. Ionization density can be determined as a function of distance along the flow tube using an axially movable Langmuir probe.[67,68] At a position downstream in the flow, photon emissions from the afterglow plasma can be observed by focusing those emissions onto the entrance slit of an optical monochromator (Action Research Corporation model AM-506), spectrally dispersed and detected by a cooled photomultiplier (Products for Research housing with an EMI 9816QB photomultiplier) followed by photon counting, by a gated photon counter (Stanford Research Systems Model SR400). A reactant gas inlet ring port facing upstream is situated just downstream of the monochromator viewing region so that the emissions can be produced in a very localized region; a He flush is added to this flow to optimize the chemistry in the emitting region. A port is located further upstream in the flow tube through which known flows of reactant gases can be pulsed to produce slugs of reactive gases in the flow; this was used in previous spectroscopic experiments to distinguish emissions from specific reactions.[69,70] In this mode, two photon counters are used one of which collect counts when the pulsed gas is absent and the other when it is present. Counting on each point in the scan is done until a predetermined signal-to-noise ratio is achieved, such that each point with signal is just as statistically accurate as the next, see Williams et al. and Mostefaoui et al. for details.[69,70] For these experiments a ~1% SF_6/He mix was pulsed into the flowtube and used to attach electrons and quench the DR process, as described previously.[70] Briefly, the difference between the SF_6 absent versus present in the flowtube, is the signal originating from the DR process, thus enabling the DR emissions to be distinguished from all other emissions. The pulsed gas port is a single tube facing upstream and located just upstream of the monochromator viewing region. The location and orientation of the pulsed gas port are such that it maximizes the mixing of the SF_6 prior to the formation of the recombining ion; thus, DR is nearly completely quenched. All of the other reactant gas ports are ring ports facing upstream so that the gas is uniformly dispersed in a small axial distance. The details of the spectroscopic techniques have recently been published.[70] In these studies Ar, H_2, and CS_2 were consectively added to the He flow as discussed in section 2.1. All of the measurements were conducted at room temperature, although the apparatus has the capability to operate between 80 and 600 K. Reactant gases were used as supplied by the manufacturer (National Welders Supply Co.) and, in all cases, were further purified by passing through molecular sieve traps at low temperature (80 K for He (99.995%) and H_2 (99.999% purity) and 200 K for Ar (99.999% purity)). CS_2 (99.9% purity) was freeze-pump-thawed several times before use.

2.1. Plasma Kinetics and Spectral Emissions. He^+ and helium metastable atoms, He^m, were produced in the discharge and studies were conducted at about 2 Torr to ensure that most of the He^+ was destroyed a short distance downstream by the association reaction

$$He^+ + He + He \rightarrow He_2^+ + He \qquad k = 1 \times 10^{-31}\ cm^6\ s^{-1} \quad (1)$$

Note that k is the reaction coefficient and is termolecular for eq 1 and bimolecular for the rest of the chemical equations. Ar was added further downstream to destroy He_2^+ and He^m by

$$He_2^+ + Ar \rightarrow Ar^+ + 2He \quad k = 2.0 \times 10^{-10}\ cm^3\ s^{-1} \quad (2)$$

$$He^m + Ar \rightarrow Ar^+ + e + He \qquad k = 7 \times 10^{-11}\ cm^3\ s^{-1}\ (ref\ 71) \quad (3)$$

creating an Ar^+/e plasma, with only a small presence of He^+, approximately 0.2% of the total ion density at the addition point of CS_2. CS_2 vapor was added to produce the recombining ion CS_2^+

$$Ar^+ + CS_2 \rightarrow S^+ + CS + Ar \qquad 93\% \qquad k = 3.7 \times 10^{-10}\ cm^3\ s^{-1}\ (ref\ 72) \quad (4)$$

$$\rightarrow CS_2^+ + Ar \qquad 7\% \quad (5)$$

Note also that S^+ reacts further by

$$S^+ + CS_2 \rightarrow S_2^+ + CS \qquad 52\% \qquad k = 1.4 \times 10^{-9}\ cm^3\ s^{-1} \quad (6)$$

$$\rightarrow CS_2^+ + S \qquad 48\% \quad (7)$$

as measured in our laboratories.[72] Note that rate coefficients (k) and the percentage product distributions were obtained from literature compilations,[73] unless otherwise indicated by a reference after the rate coefficient. S_2^+ and CS_2^+ then only react slowly with CS_2 by association and are available to recombine with electrons. Ground state S_2^+ can only recombine to give S atoms with an available energy of (4.95 eV). It is only energetically possible to produce low-lying, nonradiating states of S. These accessible states ($^1S_0$, $^1D_2$, and $^3P_{0,1,2}$) are all in the ground electronic state ($3s^23p^4$) configuration of S.

The HCS_2^+ recombining ion was produced by adding H_2 to the flow tube downstream of the Ar but prior to the CS_2, whence the reaction sequence is

$$Ar^+ + H_2 \rightarrow ArH^+ + H \quad k = 8.9 \times 10^{-10}\ cm^3\ s^{-1} \quad (8)$$

$$ArH^+ + H_2 \rightarrow H_3^+ + Ar \quad k = 6.3 \times 10^{-10}\ cm^3\ s^{-1} \quad (9)$$

$$H_3^+ + CS_2 \rightarrow HCS_2^+ + H_2 \quad k = 6.8 \times 10^{-9}\ cm^3\ s^{-1}\ (ref\ 72) \quad (10)$$

A small percentage of H_2^+ (2%) is also generated in reaction 8, but this is rapidly converted to H_3^+ by reaction with H_2.[73] For CS_2^+ and HCS_2^+ recombination, the following channels are energetically possible:

$$CS_2^+ + e \rightarrow S + CS + 5.51\ eV \quad (11)$$

$$\rightarrow C + S_2 + 2.57\ eV \quad (12)$$

and

$$HCS_2^+ + e \rightarrow H + CS_2 + 6.53\ eV \quad (13)$$

$$\rightarrow SH + CS + 7.35\ eV \quad (14)$$

$$\rightarrow CH + S_2 + 2.51\ eV \quad (15)$$

$$\rightarrow S + HCS + 4.02\ eV \quad (16)$$

but are not necessarily all significant. Energetics refer to ground state products and have been calculated using data from NIST compilations.[74] The reaction sequences producing these ions have been modeled kinetically as a function of distance along the flow tube for the neutral concentrations used in these studies, and the ion concentrations are plotted as a function of distance in Figure 1. In the CS_2^+ formation case, CS_2^+ is the dominant ion by a factor of 1.33 over S_2^+. In any case, as noted earlier, ground state S_2^+ recombination can only yield S atoms in nonradiative states. The next most abundant ion, Ar^+, is nearly 2 orders of magnitude smaller in this region and has a slow recombination rate. Thus, it is not competitive. In the HCS_2^+ case, prior to the introduction of CS_2, there is some remaining He^+, 1 order of magnitude lower than H_3^+, which can react with CS_2

$$He^+ + CS_2 \rightarrow S^+ + CS + He \quad 58\% \quad k = 2.0 \times 10^{-9}\ cm^3\ s^{-1} \quad (17)$$

$$\rightarrow CS^+ + S + He \quad 31\% \quad (18)$$

$$\rightarrow C^+ + S_2 + H \quad 11\% \quad (19)$$

The S^+ and CS^+ products react rapidly, 1.4×10^{-9} cm^3 s^{-1} and 1.3×10^{-9} cm^3 s^{-1} respectively, with CS_2 generating S_2^+ (52%) and CS_2^+ (48%) from the S^+ reaction and 100% CS_2^+ from the CS^+ reaction.[72] Even with this generation of CS_2^+, for this case, its number density is still more than 30 times less than HCS_2^+, the ion of interest, thus interfering emissions are relatively insignificant. Following the small product channel (19), the C^+ reacts with CS_2 to produce CS^+ and C^+, 91% and 9% respectively, yet these ion concentrations are insignificant compared to the magnitude of HCS_2^+. Thus, it can be seen from the modeling that HCS_2^+ is by far the dominant ion.

3. Results and Discussion

Spectral scans from the CS_2^+/e and HCS_2^+/e plasmas were acquired over the wavelength range 180−800 nm, and the wavelength regions where there were significant emissions are shown in Figures 2 and 3.

Over the range of 180−800 nm, the identified emission features are the $CS(A^1\Pi \rightarrow X^1\Sigma^+)$, $S(^5S_2^0 \rightarrow {}^3P_2)$, $S(^5S_2^0 \rightarrow {}^3P_1)$, $CS(a^3\Pi \rightarrow X^1\Sigma^+)$, $CS(B^1\Sigma^+ \rightarrow A^1\Pi)$, $CS^+(B^2\Sigma^+ \rightarrow A^2\Pi_i)$, and CS_2^+ $(\tilde{A}^2\Pi_u \rightarrow X^2\Pi_g)$. Obviously the ion emissions can only originate from ion−molecule reactions, whereas the neutral emissions can originate from these or from DR. The origins of the neutral emissions were determined in several ways. For example, for the $CS(A \rightarrow X)$ emissions, the spectrum over the wavelength range 240−290 nm was obtained, see Figure 4.

To distinguish emissions from processes involving electrons, a ∼1% mixture of SF_6 in He was pulsed into the flow tube, just upstream of reactant port 4 (CS_2 addition point), while accumulating the counts at each wavelength when the SF_6 was absent and present. When SF_6 is present, the electrons are rapidly attached to form mainly SF_6^- with a small amount of SF_5^- [75,76] and DR is quenched, thus quenching the emissions from that source. Therefore, subtraction of the counts when electrons are absent from those when electrons are present gives a spectrum due only to processes involving electrons, which in this case is limited to the DR process. Additionally, this difference (S) between SF_6 out and SF_6 pulsed in is integrated until a $S/\delta S$ of 10 is achieved, where δS is the statistical error associated with counting.[70] An example of the DR spectrum (i.e., spectrum of the difference) and integrated spectrum is shown in Figure 4.

The details of this technique have been published recently.[70] Note that when electrons are absent negative ions are present and thus ion−ion recombination can occur. Any emissions from this process would have appeared as negative going counts, which were not observed. This process is not expected to be very significant, since the recombination rate coefficients are typically 1 order of magnitude smaller than DR rate coefficients.[77] Also, less energy is available by the electron detachment energy of the negative ion, giving less chance for electronic excitation. The ion−ion recombination process is generally considered to proceed by electron transfer at long range and so would only produce the neutralized ions. However, there has been no evidence of such emissions in the region of the $CS(A \rightarrow X)$ transitions. With the amount of SF_6 added to cause rapid attachment, there would have been no significant effect on the ion chemistry, since rapid attachment coefficients are typically 2 orders of magnitude larger than for ion−molecule reactions.

To further confirm that the $CS(A \rightarrow X)$ emissions were only from DR, the discharge cavity was moved to change the upstream ionization density and thus the electron density, [e], in the flow tube. The density just upstream of the CS_2 addition point was determined using the axially movable Langmuir probe operating in the orbital limited region,[68] and the spectrum was determined at each density with a separate determination of the intensity of a series of the spectral peaks including one resulting from each v' populated. For a recombination source of the emissions, intensity is proportional to [+][e] or $[e]^2$ for a recombining ion density which is a constant fraction of [e]. The relationship between intensity and electron density is developed below:

$$\frac{d[e]}{dt} = -\alpha[e][+] = -\frac{d[product]}{dt}, \quad \text{for quasineutral plasma} \quad [e] = [+] \quad (20)$$

$$\frac{d[product]}{dt} \propto \text{intensity} \propto [e]^2 \quad (21)$$

Figure 5 shows a log−log plot of intensity versus [e] for a

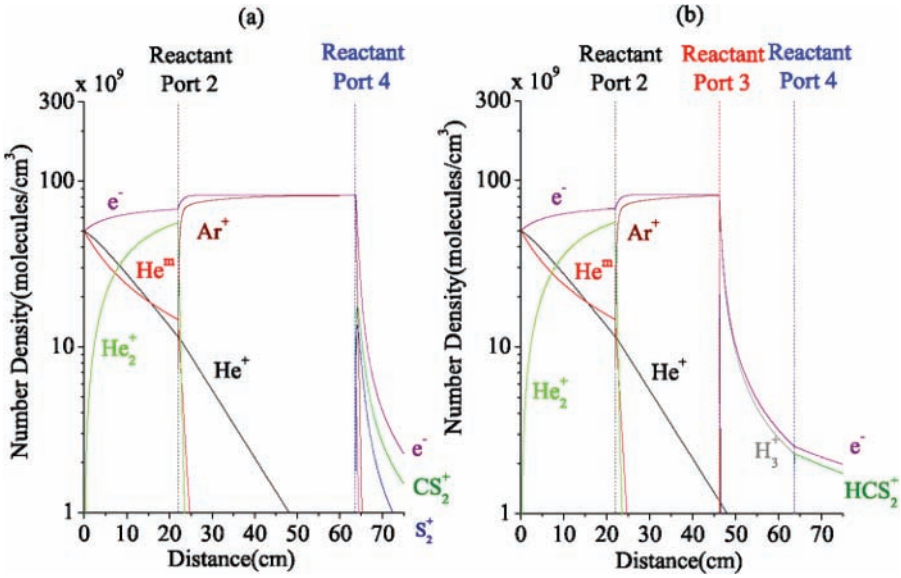

Figure 1. Kinetic modeling of the ion concentrations as a function of position along the flow tube for typical conditions under which the spectral studies were made. Distance 0 cm on the *x* axis indicates the position of the plasma source (i.e., microwave discharge) (a) For an He/Ar/CS_2 plasma and (b) for an He/Ar/H_2/CS_2 plasma. Typical neutral concentrations were [Ar] = 4.5×10^{13} molecules cm^{-3} (added at port 2), [H_2] = 1.0×10^{14} molecules cm^{-3} (added at port 3) and [CS_2] 9.0×10^{13} molecules cm^{-3} (added at port 4) with a He pressure of 2 Torr. Note that spectroscopic emissions are observed in the vicinity of the CS_2 addition point. Details of the ion concentration variations are discussed in the text.

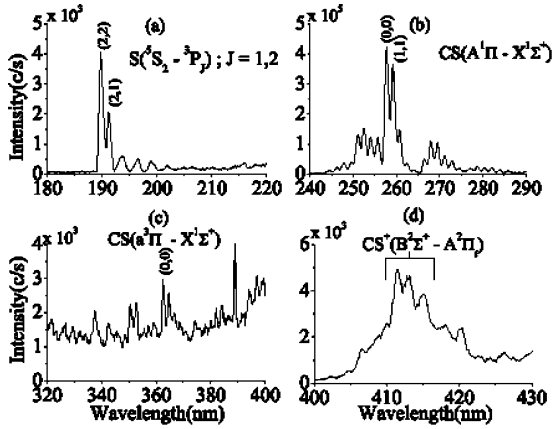

Figure 2. Spectral scans in the range of 180 to 800 nm for the CS_2^+ recombining plasma. The major emission features are indicated. These have been rescaled and plotted in four different graphs, labeled a−d corresponding to each feature on the main scan.

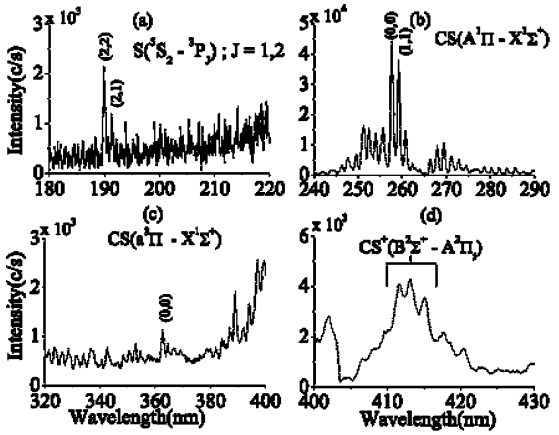

Figure 3. Spectral scans in the range of 180 to 800 nm for the HCS_2^+ recombining plasma. Illustrated are the major emission features. These have been rescaled and plotted in four different graphs, labeled a−d corresponding to each feature on the main scan.

series of vibronic transitions which is linear with a slope of 2 indicating a recombination source for the CS(A → X). Here the only possible source is reaction 11. In contrast to this, the dependence of the CS_2^+ emissions on electron density for various vibronic transitions are also shown in Figure 5. These have a slope close to one as expected for an ion−molecule reaction source ($Ar^+ + CS_2$), such as reaction 5. Note, that emissions from ion−molecule reactions are independent of the pulse valve operation. Therefore, these emissions get subtracted out from the signal (S = A − B) collect for emissions from DR products, thus are not a source of interference.

Emissions from the DR process give rise to two main electronic transitions which arise from the dominant energy channels, 11 and 14. The additional energy beyond the energy needed for electronic excitation to CS(A) and CS(a) states can go into kinetic and internal energy of the molecule. Assuming all energy goes into internal energy, the vibrational level $v' = 5$ (CS_2^+/e) and $v' = 24$ (HCS_2^+/e) of the CS(A) state can be energetically accessed. For CS(a), $v' = 17$ (CS_2^+/e) and $v' = 37$ (HCS_2^+/e) are energetically accessible. The observed vibrational levels have been identified for CS(A → X) and CS(a → X) in spectra of the CS_2^+/e and HCS_2^+/e plasmas, Figures 6 and 7.

These observed vibrational levels are all energetically accessible for both CS(A) and CS(a) states with the exception of $v' = 6$ (CS(A) state) from the CS_2^+/e plasma. This emission is relatively weak, 2% of the main (0,0) transition, but may be due to residual internal energy in CS_2^+. The residual internal energy could be quenched by the addition of excess CS_2. The extra CS_2 would react with the internally excited CS_2^+ (CS_2^+*) in a charge-transfer reaction that would leave the excess energy in the neutralized CS_2, see below:

$$CS_2^+* + CS_2 \rightarrow CS_2* + CS_2^+ \qquad (22)$$

Evidence for the above reaction could be obtained by monitoring the intensity of transitions, produced by DR, with the addition of excess CS_2. If internal excitation existed, then the intensities for the scanned transitions would change because of quenching the internal excitation and an effective reduction of the intensities

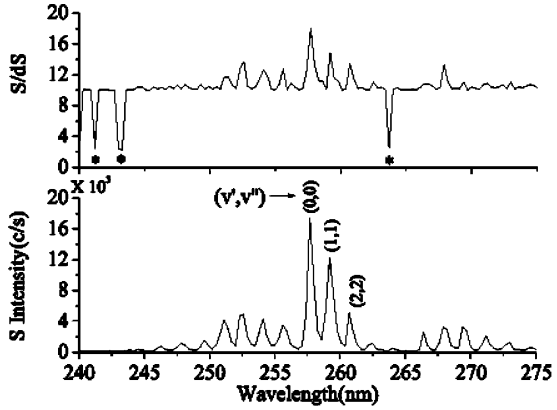

Figure 4. Shown are vibrationally resolved CS(A-X) emissions, generated following electron recombination of CS_2^+. These emissions were obtained by pulsing SF_6 into the Ar^+/e plasma upstream of the CS_2 addition point to attach electrons forming negative ions and quenching DR emissions. These emissions, *S*, are the only ones evident in this wavelength range and some of the vibrational states (v', v'') are indicated. $S/\delta S$ is also shown, which represents the constant signal-to-noise ratio in the spectrum achieved by appropriately changing the count period. In this case, photon counts have been accumulated at each wavelength until a $S/\delta S$ ratio of at least 10 was achieved. Note, * indicates where the predetermined $S/\delta S$ could not be achieved in a reasonable time because of absence of signal, thus the count was terminated.

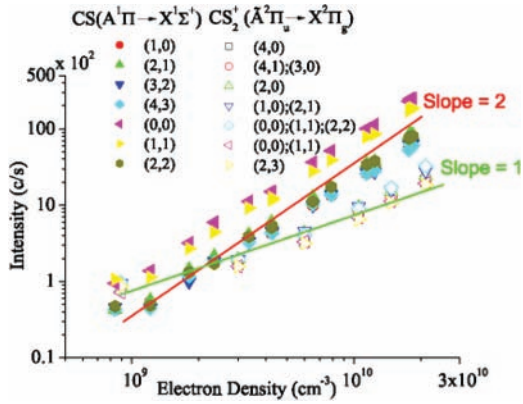

Figure 5. Intensity change due to a variation in the electron density for a series of (v', v'') transitions. The slope of the data on a log−log plot indicates the type of reaction, ion−molecule or DR, that is producing the emissions. A slope of 2 is indicative of the DR process, yielding CS(A-X) transitions. A slope of 1 is due to ion−molecule reactions, seen in the CS_2^+ (Ã-X) transitions (see section 3 for further explanation).

would be observed. This effect is not seen in Figure 8, where the CS(A → X) transitions are monitored at a CS_2 number density as used in the experimental data presented and at a number density of CS_2 that was four times larger for both CS_2^+/e and HCS_2^+/e plasmas. It can be seen that there is no change in any of the transitions indicating the absence of internal excitation. Note that, in the CS_2^+ plasma, the change is so small that the two spectra are on top of one another. The possible explanation for the occupancy of the $v' = 6$ level is that there is energetically a small percent (2%) of molecules from the $v' = 5$ level that will occupy the $v' = 6$ level. This is based on the room-temperature Boltzmann distribution for the $v' = 5$ level; therefore, emissions from the $v' = 6$ level are not surprising. The identified vibrational transitions along with available Franck−Condon factors (FCF) for the electronic transitions were used to calculate the relative vibrational distribution

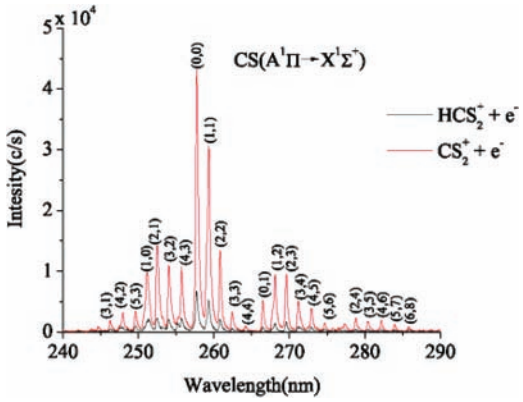

Figure 6. Major vibronic (v', v'') emission features from the CS($A^1\Pi \rightarrow X^1\Sigma^+$) transition in a CS_2^+ recombining plasma(red) and a HCS_2^+ recombining plasma(black).

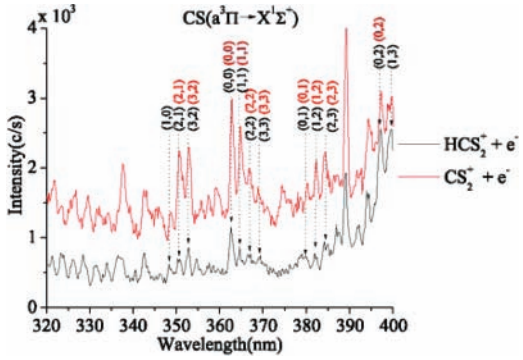

Figure 7. Major vibronic (v', v'') emission features from the CS($a^3\Pi \rightarrow X^1\Sigma^+$) transition in a CS_2^+ recombining plasma(red) and a HCS_2^+ recombining plasma(black). These features arise from a spin forbidden transition resulting in lower intensity features than those from the CS-($A^1\Pi \rightarrow X^1\Sigma^+$) transition, Figure 6.

$$I_{v'v''} \propto \nu^3 N_{v'} \mathrm{FCF} \tag{23}$$

where ν is the frequency of the transition and $N_{v'}$ is the population of vibrational level v'. These relative distributions are shown in Table 1.

For the CS(A) state, there is an increase in relative population from the $v' = 0$ to $v' = 1$ for both recombining ions. This population inversion has been observed before in previous studies where the CS($A^1\Pi \rightarrow X^1\Sigma^+$) was produced by dissociative excitation of CS_2, by electron impact[78] and by the reaction, $Ar(^3P_2) + CS_2$.[79] It is noticed that, in the HCS_2^+ recombination, the $v' = 1$ has a greater population inversion, which maybe due to the higher energy associated with this recombination. Also interesting to note is the increase in relative population going from the $v' = 3$ to $v' = 4$ (HCS_2^+), which is not observed in the CS_2^+ case. This change was not observed by Zubek et al.[78] or Xu et al.[79] The reason for this behavior is unknown to the authors. The distribution for the CS(a) state only goes to $v' = 2$ due to the lack of availability of FCF for other transitions. It is noticed that there is a population inversion that increases with increasing v' in the CS_2^+ plasma, yet this is not observed in the HCS_2^+ plasma.

The S I emissions at wavelengths of 190.04 and 191.47 nm are equivalent to a transition energy of 6.52 eV. Neither the CS_2^+ nor HCS_2^+ DR (eqs 11 and 16) have sufficient energy to produce the sulfur transitions observed. The other possible source may be an ion−molecule reaction, yet the log−log plot of intensity versus [e] has a slope of 2, which corresponds to the DR process. Note this plot is not shown to avoid repetition due to the similarities to the plot of the CS(A → X) transitions

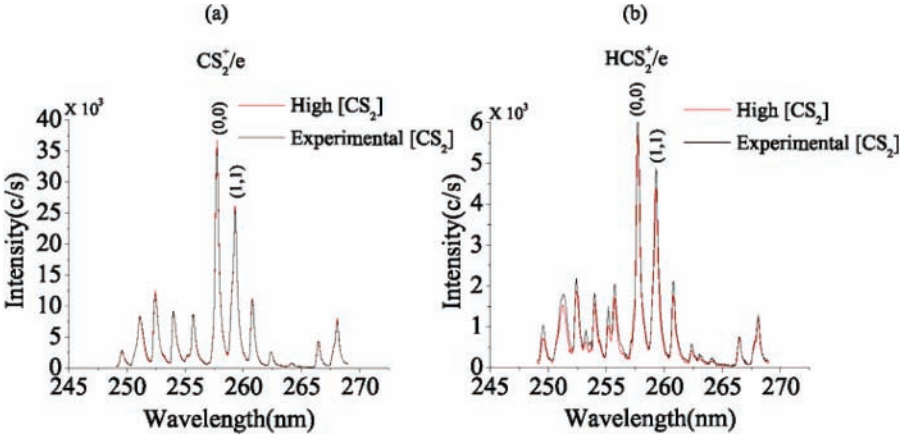

Figure 8. Spectra of CS_2^+/e recombining plasma (a) and HCS_2^+/e recombining plasma (b) taken in the region of the CS($A^1\Pi \rightarrow X^1\Sigma^+$) transition, at both a high number density (red) of CS_2 and the lower number density used in experiments (black). There is no change in intensity of the transitions between the number density used in the experiments and a number density that was four times larger. This is evidence supporting the absence of additional excitation in the recombining ion (see the text discussion referring to eq 22 for a detailed explanation).

TABLE 1: Relative Vibrational Distributions for CS($A^1\Pi \rightarrow X^1\Sigma^+$) and CS($a^3\Pi \rightarrow X^1\Sigma^+$) Transitions Originating from DR[a]

	relative distribution CS($A^1\Pi \rightarrow X^1\Sigma^+$)			relative distribution CS($a^3\Pi \rightarrow X^1\Sigma^+$)	
υ'	CS_2^+	HCS_2^+	υ'	CS_2^+	HCS_2^+
0	1.000	1.000	0	1.000	1.000
1	1.075	1.262	1	1.200	0.900
2	0.800	0.952	2	1.400	0.900
3	0.500	0.643			
4	0.500	0.762			

[a] The electronic transitions are presented for both recombining plasmas, CS_2^+/e^- and HCS_2^+/e^-. All vibrational levels are normalized to the $\upsilon' = 0$ level.

in Figure 5. Since there is no evidence for excitation in the CS_2^+ recombining ion (Figure 8), the other possibility is excitation in S_2^+. However the only source of S_2^+ is eq 6 and there is not enough energy involved to excite S_2^+ to where DR of S_2^+ will produce the emissions observed. This leaves only radiative recombination of S^+ to produce the emissions, yet this is thought of as being a very slow process. Overall there is no spectral interference from this source with the recombining ions of interest since the all radiative emissions from S atoms are at shorter wavelengths than emissions of interest (i.e., CS($A \rightarrow X$) and CS($a \rightarrow X$)).

Another transition that was identified as being due to an ion−molecule transition was the $CS^+(B^2\Sigma^+ \rightarrow A^2\Pi_i)$ in the region of 405−415 nm. The $CS^+(B^2\Sigma^+ \rightarrow A^2\Pi_i)$ vibronic transition intensities were observed to vary proportionally to the electron density on a log−log scale, similar to the CS_2^+ transitions, as expected from ion−molecule reactions. Vibronic transitions (0,0), (1,1), and (2,2) for this transition have been observed in previous work by Yencha et al.[80] In addition, the CS($B^1\Sigma^+ \rightarrow A^1\Pi$) transition has been identified in the region of 390−420 nm as well using previous work by Yencha et al.[80] Both of these transitions have been identified as coming from the $He^+ + CS_2$ reaction by Yencha et al. The comparison between the results from this study and the results from the Yencha et al. study agree that the $CS^+(B^2\Sigma^+ \rightarrow A^2\Pi_i)$ transitions are originating from ion−molecule reactions. This latter study also finds no evidence for these emissions originating from DR.

4. Conclusions

It has been shown that dominant emissions from the CS($A^1\Pi \rightarrow X^1\Sigma^+$) occur in both the CS_2^+/e and HCS_2^+/e plasmas. From these emissions relative vibrational state distributions have been assign up to the $\upsilon' = 4$ level. The increase in the population inversion for $\upsilon' = 1$ in the HCS_2^+/e plasma compared to that in the CS_2^+/e plasma is consistent with the higher energy associated with the HCS_2^+ recombination. Also consistent with the higher recombination energy are the greater relative populations in the HCS_2^+/e case than the case CS_2^+/e for $\upsilon' \geq 2$ levels. There is evidence for the vibrational transition from the $\upsilon' = 6$ in CS_2^+/e plasma, yet this is only one quantum number (0.12 eV) above the highest energetically accessible $\upsilon' = 5$ level, in which a small percentage can occupy the $\upsilon' = 6$ level from the $\upsilon' = 5$, according to the room-temperature Boltzmann distribution. Comparing spectral intensities at two CS_2 number densities, one at experimental concentration and one higher, gives no indication of internal excitation in the recombining ion, Figure 8. In addition, this vibrational level, $\upsilon' = 6$, is only 2% of the main transition. Everything being considered, it is not a strong indication of internal excitation.

The issue of cascading must be addressed, for the case of the HCS_2^+/e plasma there is enough energy to populate the singlet CS(A′, $\upsilon' \leq 7$) and the triplet CS(a′ $^3\Sigma^+$, $\upsilon' \leq 46$), CS(d $^3\Delta_i^n$, $\upsilon' \leq 26$) and CS($e^3\Sigma^-$, $\upsilon' \leq 22$) states. Starting with the CS(A′) state, there is a possible contribution to the singlet CS(A) state transitions from (υ',0), yet these were looked for and no significant peaks were observed. The next contributions considered were transitions from the triplet states, CS(a′), CS(d), and CS(e)), to the CS(a). These fall in the range from 400−800 nm for the (υ', 0) transitions. From 580−800 nm, there are no features corresponding to any of these transitions, but from 400−580 nm, it is difficult to tell due to overlapping transitions, from ion−molecule reactions. In the case of the CS_2^+ plasma, there is less energy available from the DR, thus the CS(A′) state is not accessible and the only accessible υ' levels in the triplet states are CS(a′ $^3\Sigma^+$, $\upsilon' \leq 18$), CS(d $^3\Delta_i^n$, $\upsilon' \leq 12$) and CS($e^3\Sigma^-$, $\upsilon' \leq 8$). None of the (υ', 0) transitions were observed, yet this maybe be due to unfavorable Franck−Condon factors and to the authors knowledge these are not available in the literature. Thus there are not any conclusive findings to say that these higher energy triplet states are contributing to the CS(a) state vibrational population.

In summary, it was concluded that the emissions at 190.04 and 191.47 nm were S I transitions. These transitions are associated with DR, which is possibly from radiative recombination of the S^+ ion generated in $Ar^+ + CS_2$ reaction. Next the CS ($a \rightarrow X$), which is the only spin forbidden transition

seen, yet this shows that slower emitting transitions are observed and that detection of other slow radiative decays could be obtained, yet none were observed. It should be noted that both the CS(a → X) and CS(A → X) transitions have been identified as originating from the DR, whereas the CS_2^+ ($\tilde{A} \rightarrow X$) transition has been shown to arise from ion−molecule reactions. Other transitions originating from ion−molecule reactions are the $CS^+(B^2\Sigma^+ \rightarrow A^2\Pi_i)$ and $CS(B^1\Sigma^+ \rightarrow A^1\Pi)$, presumably from the He^+ reaction with CS_2 as seen in the literature.[80]

There is evidence of CS_2 in cometary comae.[60] It is not unreasonable to assume that the protonated form, HCS_2^+, exists there also. Evidence for smaller fragments of these molecules have also been seen, making the study of the recombination of these two molecules important in determining the contribution to interstellar molecules, both neutrals and ions. This information will guide the theory of these two recombination processes and possibly give insight into determining the potential energy surfaces for these recombinations.

Acknowledgment. Support Funding from NSF Grant No. 0212368

References and Notes

(1) Herbst, E. In *Advances in Gas Phase Ion Chemistry*; Adams, N. G., Babcock, L. M., Eds.; JAI Press Ltd: Greenwich, 1998; Vol. 3, pp 1−48.

(2) Cravens, T. E. In *Dissociative Recombination of Molecular Ions with Electrons*; Guberman, S. L., Ed.; Kluwer: New York, 2003; pp 385−400.

(3) Fox, J. L. In *Dissociative Recombination Theory, Experiment and Applications II*; Rowe, B. R., Mitchell, J. B. A., Canosa, A., Eds.; Plenum: New York, 1993; p 219.

(4) Millar, T. J. In *Rate Coefficients in Astrochemistry*; Millar, T. J., Williams, D. A., Eds.; Kluwer: Dordrecht, The Netherlands, 1988.

(5) Dalgarno, A. In *Dissociative Recombination: Theory, Experiment and Applications IV*; Larsson, M., Mitchell, J. B. A., Schneider, I. E., Eds.; World Scientific: Singapore, 2000; pp 1−12.

(6) Goodings, J. M.; Karellas, N. S.; Hasanali, C. S. *Int. J. Mass Spectrom. Ion Process.* **1989**, *89*, 205−226.

(7) Post, D. E. In *Physics of Ion-Ion and Ion-Electron Collisions*; Brouillard, F., McGowan, J. W., Eds.; Plenum Press: New York, 1983; pp 37−99.

(8) Biondi, M. A. In *Recombination*; Bekefi, G., Ed.; Wiley: New York, 1976; p 125.

(9) McLain, J. L.; Poterya, V.; Jackson, D. M.; Adams, N. G.; Babcock, L. M. *J. Phys. Chem. A* **2005**, *109*, 5119−5123.

(10) McLain, J. L.; Poterya, V.; Molek, C. D.; Babcock, L. M.; Adams, N. G. *J. Phys. Chem. A* **2004**, *108*, 6704−6708.

(11) Poterya, V.; McLain, J. L.; Adams, N. G.; Babcock, L. M. *J. Chem. Phys. A* **2005**, *109*, 7181−7186.

(12) Adams, N. G.; Smith, D. In *Techniques for the Study of Ion-Molecule Reactions*; Farrar, J., Saunders, J. W., Eds.; Wiley-Interscience: New York, 1988; pp 165−220.

(13) Heber, O.; Andersen, L. H.; Seiersen, K.; Bluhme, H.; Svendsen, A.; Maunoury, L. In Wolf, A., Ed., *Sixth International Conference on Dissociative Recombination: Theory, Experiments and Applications, Mosbach, Germany*, 2004.

(14) Thomas, R. D.; Ehlerding, A.; Geppert, W.; Hellberg, F.; Larsson, M.; Zhaunerchyk, V.; Bahati, E.; Bannister, M. E.; Vane, C. R.; Petrignani, A.; van der Zande, W. J.; Andersson, P.; Pettersson, J. C., Wolf, A., Lammich, L., Schmelcher, P., Eds.; Institute of Physics: London, 2005; J. Phys. Conf. Series 4, pp 187−190.

(15) Mitchell, J. B. A.; Rebrion-Rowe, C.; Le Garrec, J. L.; Angelova, G.; Bluhme, H.; Seiersen, K.; Andersen, L. H. *Int. J. Mass Spectrom.* **2003**, *227*, 273−9.

(16) Kalhori, S.; Viggiano, A. A.; Arnold, S. T.; Rosen, S.; Semaniak, J.; Derkatch, A. M.; af Ugglas, M.; Larsson, M. *Astron. Astrophys.* **2002**, *391*, 1159−1165.

(17) Andersen, L. H.; Heber, O.; Kella, D.; Pedersen, H. B.; Vejby-Christensen, L.; Zajfman, D. *Phys. Rev. Lett.* **1996**, *77*, 4891−4.

(18) Rosen, S.; Derkatch, A. M.; Semaniak, J.; Neau, A.; Al-Khalili, A.; Le Padellec, A.; Vikor, W. S. L.; Thomas, R.; Danared, H.; af Ugglas, M.; Larsson, M. *Faraday Discuss.* **2000**, *115*, 295−302.

(19) Petrignani, A.; Hellberg, F.; Thomas, R. D.; Larsson, M.; Cosby, P. C.; van der Zande, W. J. In *Dissociative Recombination, Theory, Experiments and Applications*; Wolf, A., Lammich, L., Schmelcher, P., Eds.; Institute of Physics: London, 2005; J. Phys. Conf. Series 4, pp 182−186.

(20) Rowe, B. R.; Queffelec, J. L. In *Dissociative Recombination: Theory, Experiment and Applications*; Mitchell, J. B. A., Guberman, S. L., Eds.; World Scientific: Singapore, 1989; pp 151−61.

(21) Queffelec, J. L.; Rowe, B. R.; Vallee, F.; Gomet, J. C.; Morlais, M. *J. Chem. Phys.* **1989**, *91*, 5335−42.

(22) Adams, N. G.; Herd, C. R.; Geoghegan, M.; Smith, D.; Canosa, A.; Gomet, J. C.; Rowe, B. R.; Queffelec, J. L.; Morlais, M. *J. Chem. Phys.* **1991**, *94*, 4852−4857.

(23) Queffelec, J. L.; Rowe, B. R.; Morlais, M.; Gomet, J. C.; Vallee, F. *Planet. Space Sci.* **1985**, *33*, 263−270.

(24) Vallee, F.; Gomet, J. C.; Rowe, B. R.; Queffelec, J. L.; Morlais, M. In *Astrochemistry*; Varda, M. S., Tarafdar, S., Eds.; Kluwer: Dordrecht, 1987; pp 29−30.

(25) Rowe, B. R.; Vallee, F.; Queffelec, J. L.; Gomet, J. C.; Morlais, M. *J. Chem. Phys.* **1988**, *88*, 845−850.

(26) Vejby-Christensen, L.; Andersen, L. H.; Heber, O.; Kella, D.; Pedersen, H. B.; Schmidt, H. T.; Zajfman, D. *Astrophys. J.* **1997**, *483*, 531−540.

(27) Jensen, M. J.; Bilodeau, R. C.; Heber, O.; Pedersen, H. B.; Safvan, C. P.; Urbain, X.; Zaijman, D.; Andersen, L. H. *Phys Rev. A* **1999**, 60, 2970−6.

(28) Vikor, W. S. L.; Al-Khalili, A.; Danared, H.; Djuric, N.; Dunn, G. H.; Larson, A.; Le Padellec, A.; Rosen, S.; af Ugglas, M. *Astron. Astrophys.* **1999**, *344*, 1027−33.

(29) Larson, A.; Le Padellec, A.; Semaniak, J.; Stromholm, C.; Larsson, M.; Rosen, S.; Peverall, R.; Danared, H.; Djuric, N.; Dunn, G. H.; Datz, S. *Astrophys. J.* **1998**, *505*, 459−65.

(30) Derkatch, A. M.; Al-Khalili, A.; Vikor, W. S. L.; Neau, A.; Shi, W.; af Ugglas, M.; Larsson, M. *J. Phys. B* **1999**, *32*, 3391−8.

(31) Semaniak, J.; Minaev, B. F.; Derkatch, A. M.; Hellberg, F.; Neau, A.; Rosen, S.; Thomas, R.; Larsson, M.; Danared, H.; Paal, A.; af Ugglas, M. *Astrophys. J. Suppl.* **2001**, *135*, 275−83.

(32) Williams, T. L.; Adams, N. G.; Babcock, L. M.; Herd, C. R.; Geoghegan, M. *Mon. Not. R. Astron. Soc.* **1996**, *282*, 413−420.

(33) Neau, A.; Khalili, A. A.; Rosen, S.; Le Padellec, A.; Derkatch, A. M.; Vikor, W. S. L.; Semaniak, J.; Thomas, R.; Nagard, M. B.; Anderson, K.; Danared, H.; af Ugglas, M. *J. Chem. Phys.* **2000**, *113*, 1762−1770.

(34) Jensen, M. J.; Bilodeau, R. C.; Safvan, C. P.; Seiersen, K.; Andersen, L. H.; Pedersen, H. B.; Heber, O. *Astrophys. J.* **2000**, *543*, 764−774.

(35) Semaniak, J.; Larson, A.; Le Padellec, A.; Stromholm, C.; Larsson, M.; Rosen, S.; Peverall, R.; Danared, H.; Djuric, N.; Dunn, G. H.; Datz, S. *Astrophys. J.* **1998**, *498*, 886−95.

(36) Ehlerding, A.; Arnold, S.; Viggiano, A. A.; Kalhori, S.; Semaniak, J.; Derkatch, A.; Rosén, S.; af Ugglas, M.; Larsson, M. *J. Phys. Chem. A* **2003**, *107*, 2179−2189.

(37) Geppert, W. D.; Thomas, R. D.; Ehlerding, A.; Hellberg, F.; Osterdahl, F.; Hamberg, M.; Semaniak, J.; Zhaunerchyk, V.; Kaminska, M.; Kallberg, A.; Paal, A.; Larsson, M. In *Dissociative Recombination: Theory, Experiments and Applications*; Wolf, W., Lammich, L., Schmelcher, P., Eds.; Institute of Physics: London, 2005; J. Phys. Conf. Series 4, Vol. 4, pp 26−31.

(38) Geppert, W.; Thomas, R.; Semaniak, J.; Ehlerding, A.; Millar, T. J.; Osterdahl, F.; Ugglas, M. a.; Djuric, N.; Paal, A.; Larsson, M. *Astrophys. J.* **2004**, *609*, 459−464.

(39) Zhaunerchyk, V.; Ehlerding, A.; Viggiano, A. A.; Arnold, S. T.; Geppert, W. D.; Hellberg, F.; Thomas, R.; Osterdahl, F.; Larsson, M. In Wolf, A., Lammich, L., Schmelcher, P., Eds., *Sixth International Conference on Dissociative Recombination: Theory, Experiments and Applications, Mosbach, Germany*, 2004.

(40) Hamberg, M.; Geppert, W. D.; Rosen, S.; Ehlerding, A.; Hellberg, F.; Zhaunerchyk, V.; Kaminska, M.; Thomas, R.; Kallberg, A.; Simonsson, A.; Paal, A.; Larsson, M. In Wolf, A., Ed., *Sixth International Conference on Dissociative Recombination: Theory, Experiments and Applications, Mosbach, Germany*, 2004.

(41) Hellberg, F.; Zhaunerchyk, V.; Bannister, M. E.; Ehlerding, A.; Geppert, W.; Larsson, M.; Vane, C. R.; Osterdahl, F.; Thomas, R. In Wolf, A., Ed., Sixth *International Conference on Dissociative Recombination: Theory, Experiments and Applications, Mosbach, Germany*, 2004.

(42) Datz, S.; Larsson, M.; Stromholm, C.; Sundstrom, G.; Zengin, V.; Danared, H.; Kallberg, A.; af Ugglas, M. *Phys. Rev. A* **1995**, *52*, 2901−9.

(43) Datz, S.; Sundstrom, G.; Biedermann, G.; Brostrom, L.; Danared, H.; Mannervik, S.; Mowat, J. R.; Larsson, M. *Phys. Rev. Lett.* **1995**, *74*, 896−9.

(44) Johnsen, R.; Skrzypkowski, M.; Gougousi, T.; Golde, M. F. In *Dissociative Recombination: Theory, Experiment and Applications IV*; Larsson, M., Mitchell, J. B. A., Schneider, I. E., Eds.; World Scientific: Singapore, 2000; p 200.

(45) Adams, N. G.; Babcock, L. M. *J. Phys. Chem.* **1994**, *98*, 4564−4569.

(46) Butler, J. M.; Babcock, L. M.; Adams, N. G. *Mol. Phys.* **1997**, *91*, 81−90.

(47) Bates, D. R. *Adv. Atom. Mol. Opt. Phys.* **1994**, *34*, 427−486.
(48) Bates, D. R. *J. Phys. B* **1992**, *25*, 5479−5488.
(49) Bates, D. R. *Proc. R. Soc. London* **1993**, *443*, 257−264.
(50) Talbi, D. *Chem. Phys.* **2007**, *332*, 298−303.
(51) Rosati, R.; Johnsen, R.; Golde, M. F. *J. Chem. Phys.* **2004**, *120*, 8025−30.
(52) Kraemer, W. P.; Hazi, A. U. In *Dissociative Recombination: Theory, Experiment and Applications I.*; Mitchell, J. B. A.; Guberman, S. L., Eds.; World Scientific: Singapore, 1989; pp 61−72.
(53) Talbi, D.; Ellinger, Y. In *Dissociative Recombination: Theory, Experiment and Applications II*; Rowe, B. R., Mitchell, J. B. A., Canosa, A., Eds.; Plenum: New York, 1993; pp 59−66.
(54) Tomashevsky, M.; Herbst, E.; Kraemer, W. P. *Astrosphys. J.* **1998**, *498*, 728−734.
(55) Glinski, R. J.; Nuth, J. A.; Reese, M. D.; Sitko, M. *Astrophys. J.* **1996**, *467*, L109−112.
(56) Yan, M.; Dalgarno, A.; Klemperer, W.; Miller, A. E. S. *Mon. Not. R. Astron. Soc.* **2000**, *313*, L17−18.
(57) Adams, N. G.; Babcock, L. M.; Ray, N. S. In *Atomic Processes in Plasmas*; Schultz, D. R., Meyer, F. W., Ownby, F., Eds.; AIP: Melville, NY, 2002; pp 182−193.
(58) McCarthy, M. C.; Thaddeus, P. *Chem. Soc. Rev.* **2001**, *30*, 177−185.
(59) Thaddeus, P.; McCarthy, M. C. *Spectrochim. Acta* **2001**, *A57*, 757−774.
(60) Jackson, W. M.; Scodinu, A.; Xu, D.; Cochran, A. L. *Astrophys. J.* **2004**, *607*, L139−L141.
(61) Crovisier, J.; Encrenaz, T. *Comet Science;* Cambridge University Press: Cambridge, 2000.
(62) Gutcheck, R. A.; Zipf, E. C. *J. Geophys. Res.* **1973**, *78*, 5429−36.
(63) Vallee, F.; Rowe, B. R.; Gomet, J. C.; Queffelec, J. L.; Morlais, M. *Chem. Phys. Lett.* **1986**, *124*, 317−20.
(64) Tsuji, M.; Nakamura, M.; Nishimura, Y.; Obase, H. *J. Chem. Phys.* **1995**, *103*, 1413−21.
(65) Adams, N. G. In *Dissociative Recombination: Theory, Experiment and Applications*; Rowe, B. R., Mitchell, J. B. A., Eds.; Plenum Press: New York, 1993; pp 99−111.
(66) Adams, N. G.; Smith, D. *Int. J. Mass Spectrom. Ion Phys.* **1976**, *21*, 349−59.
(67) Adams, N. G. *Int. J. Mass Spectrom. Ion Proc.* **1994**, *132*, 1−27.
(68) Swift, J. D.; Schwar, M. J. R. *Electrical Probes for Plasma Diagnostics*; Iliffe: London, 1970.
(69) Williams, T. L.; Decker, B. K.; Adams, N. G.; Babcock, L. M.; Harland, P. W. *Rev. Sci. Instrum.* **2000**, *71*, 2169−79.
(70) Mostefaoui, T.; Adams, N. G.; Babcock, L. M. *Rev. Sci. Instrum.* **2002**, *73*, 2044−50.
(71) Schmeltekopf, A. L.; Fehsenfeld, F. C. *J. Chem. Phys.* **1970**, *53*, 3173−3177.
(72) Molek, C. D.; McLain, J. L.; Adams, N. G.; Babcock, L. M.; Gibbs, L. L. *Int. J. Mass Spectrom.* **2004**, *235*, 199−205.
(73) Anicich, V. *An Index of the Literature for Bimolecular Gas Phase Cation-Molecule Reaction Kinetics: JPL Publication 03−19*; Jet Propulsion Laboratory: Pasadena, CA, 2003.
(74) Linstrom, P. J., Mallard, W. G., Eds.; *NIST Chemistry WebBook*, NIST Standard Database 69; National Institute of Standards and Technology: Gaithersburg, MD; June 2005.
(75) Fehsenfeld, F. C. *J. Chem. Phys.* **1970**, *53*, 2000−2004.
(76) Smith, D.; Adams, N. G.; Alge, E. *J. Phys. B* **1984**, *17*, 461−472.
(77) Adams, N. G.; Babcock, L. M.; Molek, C. D. In *Encyclopedia of Mass Spectrometry: Theory and Ion Chemistry, Vol. 1*; Armentrout, P., Ed.; Elsevier: Amsterdam, 2003; Vol. 1, pp 555−561.
(78) Zubek, M.; Gackowska, J.; Snegursky, A. *Radiat. Phys. Chem.* **2003**, *68*, 323−328.
(79) Xu, D.; Li, X.; Shen, G.; Wang, L.; Chen, H.; Lou, N. *Chem. Phys. Lett.* **1993**, *210*, 315−321.
(80) Yencha, A. J.; Wu, K. T. *Chem. Phys.* **1980**, *49*, 127−137.